# The Raman spectrum and lattice parameters of $MgB_2$ as a function of temperature



2004 J. Phys.: Condens. Matter 16 6541

(http://iopscience.iop.org/0953-8984/16/36/019)

INSTITUTE OF PHYSICS PUBLISHING JOURNAL OF PHYSICS: CONDENSED MATTER

J. Phys.: Condens. Matter **16** (2004) 6541–6550 PII: S0953-8984(04)82461-5

# The Raman spectrum and lattice parameters of $MgB_2$ as a function of temperature

**Lei Shi[1], Huarong Zhang[1], Lin Chen[1] and Yong Feng[2]**

[1] Structure Research Laboratory, University of Science and Technology of China, Academia Sinica, Hefei, Anhui 230026, People's Republic of China
[2] Northwest Institute for Nonferrous Metal Research, PO Box 51, Xi'an 710016, People's Republic of China

Received 21 June 2004, in final form 6 August 2004
Published 27 August 2004
Online at stacks.iop.org/JPhysCM/16/6541
doi:10.1088/0953-8984/16/36/019

**Abstract**

The temperature dependences of the Raman spectrum and lattice parameters of polycrystalline $MgB_2$ have been investigated by means of Raman spectroscopy and x-ray diffraction. It is found that the lattice parameters show an approximately linear change with the temperature decrease, giving different thermal expansions along the *a*- and *c*-axes, which is caused by the comparatively weak metal–boron bonding in $MgB_2$. The grain size of $MgB_2$ determined by means of x-ray diffraction is around 45 nm for both [100] and [001] directions. There is no evidence for any structural transition while the temperature changes from 300 K down to 12 K. An anomalous Raman band at 603 $cm^{-1}$ is observed, which is consistent with the theoretical prediction for the $E_{2g}$ in-plane boron stretching mode. The Raman frequency increases and the linewidth decreases as the temperature decreases. A possible origin of the temperature dependences of the Raman frequency and the linewidth is discussed. It is suggested that the grain size effect of $MgB_2$ on the nanometric scale will have a clear influence on the frequency and the linewidth of the Raman spectrum.

## 1. Introduction

The newly discovered superconductor $MgB_2$, a binary intermetallic compound with a superconducting transition temperature of 39 K [1], has attracted considerable interest from theoretical and experimental points of view since $MgB_2$ has achieved a record high $T_c$ in the conventional superconductors. Theory indicates that $MgB_2$ can be treated as a phonon mediated superconductor with very strong coupling [2–4]. Photoemission spectroscopy [5], tunnelling spectroscopy [6], isotope effect measurements [7, 8], and inelastic neutron scattering measurements [9] also support the notion that $MgB_2$ is an electron–phonon mediated

  

conventional BCS superconductor with s-wave symmetry. However, the results of the Hall effect measurements [10] on this compound are reported to be unconventional and show good agreement with ones for high $T_c$ cuprate materials, suggesting that the B–B layers in $MgB_2$, like the Cu–O planes in cuprates, play an important role in the electrical transport properties. Some early experimental studies have indicated that $MgB_2$ has two or more superconducting gaps with different sizes develop simultaneously at $T_c$ between the occupied and unoccupied electronic states [11–13]. Gonnelli *et al* [14] and Bugoslarsky *et al* [15] have studied the structure of the superconducting gap in $MgB_2$ single crystals and films by means of point-contact spectroscopy using Au or Pt tips, proving directly the existence of a multi-valued order parameter of $MgB_2$, with two distinct values of the gap, $\Delta_1 = 7.1 \pm 0.1$ meV and $\Delta_2 = 2.8 \pm 0.05$ meV at 4.6 K in $MgB_2$ single crystals, and $\Delta_1 = 6.2 \pm 0.7$ meV and $\Delta_2 = 2.3 \pm 0.3$ meV at 4.2 K in $MgB_2$ films. Choi *et al* [16] reported an *ab initio* calculation of the gaps in $MgB_2$ and suggested that the electronic states at the Fermi level are mainly either $\sigma$ or $\pi$ bonding boron orbitals, which coincides with the experimental results of high resolution angle-resolved photoemission spectroscopy (ARPES) [13]. The strong coupling of the $\sigma$ bonding states to the in-plane vibration of boron atoms results in strong electron-pair formation of $\sigma$ bonding states, which is the principal contribution to the superconductivity, with an average energy gap $\Delta$ of 6.8 meV. The $\pi$ bonding states on the remaining parts of the Fermi surface form much weaker pairs; this is enhanced by the coupling to the $\sigma$ bonding states, with an average energy gap $\Delta$ of 1.8 meV.

On the other hand, calculations also show that the strongest coupling is realized for the near-zone-centre in-plane optical phonon ($E_{2g}$ symmetry) related to vibrations of the B atoms, which is very anharmonic because of its strong coupling to the partially occupied planar B $\sigma$ bands near the Fermi surface [2–4]. The frequency of this phonon ranges from 460 to 660 $cm^{-1}$ according to different computation techniques [2–4]. Because Raman spectroscopy is an effective technique for studying the electron–phonon interaction and the superconducting gap in superconductors [17], many Raman experiments have been carried out for $MgB_2$ superconductor. Although a broad asymmetric Raman peak near 600 $cm^{-1}$ has been observed by many research groups, the position of the Raman peak and its assignment vary depending on the research group. For example, the position of the Raman peak reported by Bohnen *et al* [18] for a 10 $\mu$m size crystalline grain is 580 $cm^{-1}$, while Chen *et al* [11] show that the position of the Raman peak at temperatures of 15 and 45 K taken from polycrystalline $MgB_2$ samples with 0.15–0.3 $\mu$m size grains is 620 $cm^{-1}$. Kunc *et al* [19] have studied the Raman spectra and the optical reflectance of $MgB_2$ as a function of pressure and argued that the dominant Raman peak near 600 $cm^{-1}$ in the ambient pressure spectra does not originate from $MgB_2$, but from a contaminant phase present at the sample surface. However, Raman spectra and the synchrotron x-ray diffraction of polycrystalline $MgB_2$ under high pressure up to 57 GPa have suggested [20, 21] that the band and its pressure dependence can be interpreted as the $E_{2g}$ zone centre phonon, which is strongly anharmonic because of coupling to electronic excitations. This also rules out another alternative interpretation of the 600 $cm^{-1}$ peak, disorder-induced scattering, as proposed in [11].

In this paper, we have investigated the temperature dependences of the Raman spectrum and lattice parameters of polycrystalline $MgB_2$. It is found that the lattice parameters show an approximately linear change with the temperature decreasing, giving different thermal expansions along the *a*- and *c*-axes, which is caused by the comparatively weak metal–boron bonding in $MgB_2$. The grain size of $MgB_2$ determined by means of x-ray diffraction is around 45 nm for both [100] and [001] directions. There is no evidence for any structural transition while the temperature goes from 300 K down to 12 K. An anomalous Raman band at 603 $cm^{-1}$ is observed, which is consistent with the theoretical prediction for the $E_{2g}$ in-plane

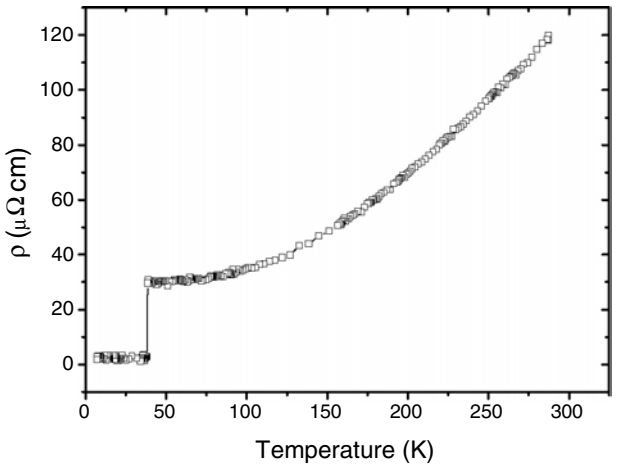


**Figure 1.** Resistivity against temperature for $MgB_2$.

boron stretching mode. The frequency increases and the linewidth decreases as the temperature decreases. A possible origin of the temperature dependences of the frequency and the linewidth has been discussed.

## 2. Experimental details

The polycrystalline $MgB_2$ superconductor was synthesized by the Mg diffusion method. Stoichiometric amounts of Mg powder (>99.5% wt% purity, 100–200 mesh, Shanghai Chemical Co. Ltd) and B powder (>99.99% wt% purity, 325 mesh, Alfa Aesar) were mixed together and pressed into pellets. The pellet was wrapped in a Ta foil, which was then sealed in a quartz ampoule under vacuum. The samples were slowly heated up to 600 °C and maintained at this temperature for 1 h, then heated up to 900 °C and maintained at this temperature for 3 h, and eventually cooled down in the furnace.

The crystal structure of $MgB_2$ was characterized by an 18 kW rotating anode x-ray diffractometer (XRD, type MXP18AHF, MAC Science) with graphite monochromatized Cu K$\alpha$ ($\lambda = 1.540\,18$ Å) radiation in the Bragg–Brentano geometry at room temperature and low temperature down to 12 K. The x-ray powder diffraction data were collected in the range 20°–115° of $2\theta$. The full pattern was fitted and the crystal structure of $MgB_2$ was modified by the Rietveld method [22]. Morphology and size information on $MgB_2$ were obtained using a JEOL (Model JSM-6700F) field emission scanning electron microanalyser (SEM). The temperature dependence of the resistivity of the sample was measured by a four-probe method from 16 to 300 K. The low temperature Raman spectra of $MgB_2$ were measured using a Spex RAMALOG6 Raman spectroscope, using a backscattering technique within the temperature range 83–293 K. The 5145 Å line from an argon-ion laser was used as an excitation light source. Several samples were chosen for the above experiments and the same results were obtained in all cases.

## 3. Results and discussion

Figure 1 shows the typical temperature dependence of the resistivity of the samples, which shows a superconducting transition $T_c$ at 38.3 K with a $\Delta T_c = 0.34$ K. The XRD pattern (figure 2) of the sample indicated that the main phase is $MgB_2$ with a minor impurity of MgO, which is the most common impurity seen in all preparations [23, 24]. The temperature

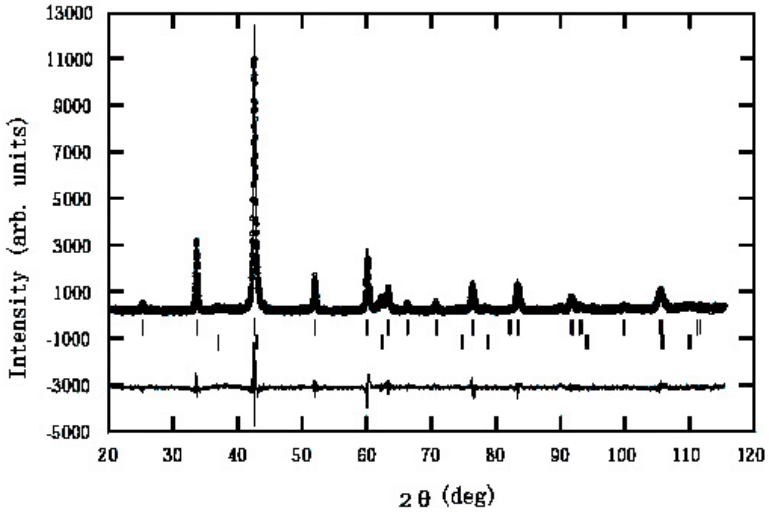


**Figure 2.** Final observed (points) and calculated (continuous curve) profiles for x-ray powder diffraction data of $MgB_2$ at room temperature (300 K). The vertical markers show positions calculated for Bragg reflections: high for $MgB_2$ ($P6/mmm$) and low for MgO ($Fm3m$). At the bottom is a plot of the difference between observation and calculation.

dependence of the XRD data analysed by the Rietveld technique revealed that the crystal structure of $MgB_2$ is an $AlB_2$-type structure, as reported in [25], with hexagonal space group $P6/mmm$ (No 191) with unit cell dimensions $a = 3.0799(5)$, $c = 3.5205(3)$ Å, $V = 28.921$ Å$^3$ at room temperature. The final values of the $R$-factors were Bragg $R$-factor $= 7.23\%$ and $R_F$-factor $= 5.68\%$. In the structure of $MgB_2$, the boron atoms form graphite-like honeycomb layers, and the magnesium atoms are located above the centre of the hexagons in between the boron planes. There is no evidence for any structural transition while the temperature goes from 300 K down to 12 K.

It should be noted that the XRD peaks in figure 2 are too broad for recognizing the K$\alpha_1$ and K$\alpha_2$ doublet even when the diffraction angle $2\theta$ is higher than 70°. After careful comparison, one can find similar results shown in the XRD patterns of other reported works, e.g. for bulk material [1, 7] and a film [26]. It is known that the peak broadening can be induced by changing grain size. To judge the grain size, a doublet with Miller indices (100) and (001) was used for the half-width analysis. The width of the reflection profiles was determined by fitting the Voigt function to the XRD pattern and, after removing the instrumental broadening from the observed line profile, the grain size was calculated from the known Scherrer equation:

$$d = \frac{\lambda}{\Delta(2\theta)\cos\theta}$$

where $d$ is the average nanocrystal diameter, $\lambda$ is the x-ray wavelength, $\Delta(2\theta)$ is the diffraction peak half-width, and $\theta$ is the diffraction angle. The thus-obtained average grain size is about 45 nm for both [100] and [001] directions. This result was confirmed by the SEM observation (see figure 3) which shows that the $MgB_2$ is a nanometric crystalline powder. Because the grain size of $MgB_2$ is on the nanometric scale, the grain size effect will play an important role in the Raman scattering (see the discussion below).

The temperature dependences of the lattice parameters and unit cell volume of $MgB_2$ are shown in figure 4. The thermal expansion can be nicely modelled with an Einstein equation

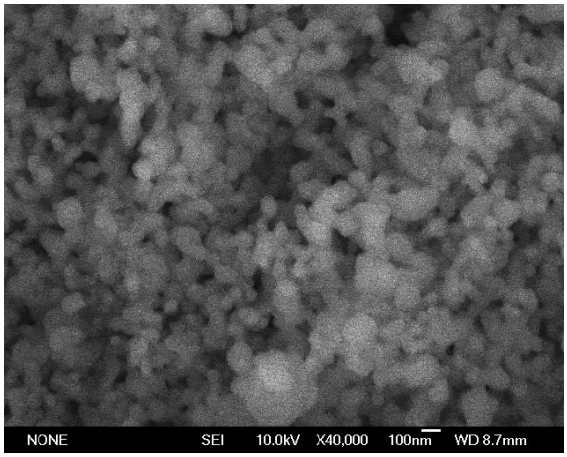


**Figure 3.** A typical SEM image of $MgB_2$.

using a single phonon energy as obtained by the neutron powder diffraction [27]:

$$\ln\left(\frac{a}{a_0}\right) = \frac{A\theta_p}{e^{(\theta_p/T)} - 1} \tag{1}$$

where $a$ is the lattice parameter ($a$ or $c$) or unit cell volume $V$ and $a_0$ is its value at $T = 0$ K, $\theta_p$ is the phonon energy, $T$ is the temperature, and $A$ is a scaling coefficient. The data of figure 4 have been fitted with this equation to determine the values of $a_0$, $A$, and $\theta_p$. Independent fits to $a$, $c$, and $V$ give the same phonon energy, $\theta_p$, within the standard deviations: 428(94), 400(51), and 420(78) K for the fits to $a$, $c$, and $V$, respectively.

From figure 4, it can be found that the lattice parameters $a$ and $c$ show an approximately linear change with the temperature decreasing from room temperature to 180 K. After fitting the thermal expansions along the $a$- and $c$-axes, linear thermal expansions in the temperature range from 180 to 300 K are obtained, which give $\alpha_a = 7.984 \times 10^{-6}\,K^{-1}$ and $\alpha_c = 7.679 \times 10^{-6}\,K^{-1}$ (where $\alpha$ is defined as $(\Delta l/\Delta T)/l_0$). The thermal expansion of $MgB_2$ lies generally within the range observed for other hexagonal diborides [28]. Besides this, the temperature dependence of the lattice parameter $c/a$ ratio ($\approx$1.1430(5) Å) remains almost unchanged within the standard deviation over the whole observed temperature range. These results reveal the three-dimensional character of $MgB_2$, which coincides with the result reported by Vogt *et al* [29]. The small difference of $\alpha_a$ and $\alpha_c$ results from the anisotropy in B–B bond strengths. In $MgB_2$, the B–B bonds in the basal plane are much stronger than the Mg–B bonds that connect layers of Mg and B atoms, which reveals a weak two-dimensional character of $MgB_2$. However, the intralayer bonds are only twice as short as the interlayer ones, allowing for a significant interlayer hopping. These results coincide with the electronic structure features of $MgB_2$. The peculiar and unique feature of $MgB_2$ is the incomplete filling of the two $\sigma$ bands corresponding to strongly covalent, $sp^2$-hybrid bonding within the graphite-like boron layer. The holes at the top of these $\sigma$ bands notably manifest two-dimensional properties and are localized within the boron sheets, in contrast with the mostly three-dimensional electrons and holes in the $\pi$ bands, which are delocalized over the whole crystal. These two-dimensional covalent and three-dimensional metallic-type states contribute almost equally to the total density of states at the Fermi level, while the unfilled covalent bands experience strong interaction with longitudinal vibrations in the boron layer.

The temperature dependence of the Raman spectrum is shown in figure 5. Clearly, there are no well-defined phonon lines in the spectra. Instead, a broad maximum centred at about 600 $cm^{-1}$ appears in the spectra and the position gradually moves up as the

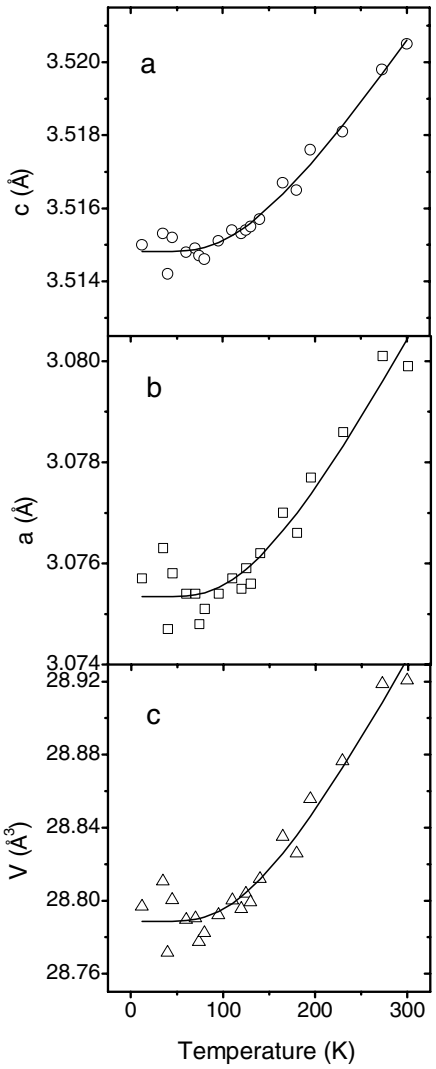


**Figure 4.** Experimental temperature dependences of the lattice parameters $a$, $c$ and unit cell volume $V$ of $MgB_2$ based on x-ray powder diffraction measurements. The solid curves are least-squares fits using a simple Einstein model with a single phonon energy (equation (1) in the text).

temperature decreases. A factor-group analysis [19] yields the decomposition of the coordinate representation for $MgB_2$ (space group $P6/mmm$, $z = 1$) as $B_{1g} + E_{2g} + 2A_{2u} + 2E_{1u}$ (at the $\Gamma$ point) and $A_{1g} + E_{1g} + A_{2u} + B_{2u} + E_{1u} + E_{2u}$ (at the A point). Of the zone centre optical models, the $A_{2u}$ mode (B and Mg planes moving against each other) and $E_{1u}$ mode (B and Mg planes sliding along $x$, $y$) are infrared active, the $B_{1g}$ mode (two borons displaced along $z$ in opposite directions) is silent, and only the $E_{2g}$ mode (in-plane displacements of borons) is Raman active. Thus it is natural to assign the band observed at about 600 $cm^{-1}$ at ambient conditions to the $E_{2g}$ mode [18, 20]. In fact, attempts to ascribe the mode observed to impurities [19] contradict polarization measurements on small single crystals [30]. These observations also rule out another alternative interpretation of the 600 $cm^{-1}$ peak, disorder-induced scattering, as proposed in [11].

To further investigate the Raman spectrum changes for $MgB_2$, the temperature dependence of the Raman spectra was fitted with a combination of a linear background and a Gaussian peak (fitting with a Lorentzian peak gives almost the same results and a similar quality of

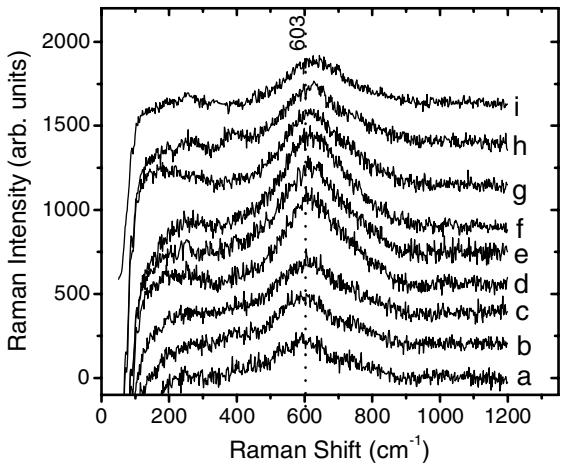


**Figure 5.** Raman spectra of $MgB_2$ at different temperatures (after subtracting the background): (a) 293 K; (b) 253 K; (c) 193 K; (d) 163 K; (e) 153 K; (f) 143 K; (g) 133 K; (h) 123 K; (i) 83 K.

fitting). Figure 6 shows fitting results for $MgB_2$ at 293 and 83 K. The frequency and linewidth (the full width at half-maximum) of the $E_{2g}$ peak determined by this procedure are plotted as a function of temperature in figure 7. From figure 7, it can be found that the temperature dependence of the measured linewidth decreases from 222 $cm^{-1}$ to about 195 $cm^{-1}$ in going from 293 to 83 K. Although the trend of the temperature-dependent linewidth change is the same, this result is in general smaller than the results of [31], in which the linewidth decreases from 300 $cm^{-1}$ to about 230 $cm^{-1}$ in going from room temperature to 5 K. The linewidth is a fundamental quantity which provides information about the two main damping mechanisms in materials: (a) orientational change in molecules [32] and (b) anharmonicity of vibrations [33]. This can be summarized in an expression such as the following:

$$\Gamma = A + BT + \Gamma_0 \exp(-E_a/k_B T) \tag{2}$$

where $\Gamma$ is the band linewidth, $A$, $B$, and $\Gamma_0$ are constants, $E_a$ is the activation energy, $k_B$ is the Boltzmann constant, and $T$ is the absolute temperature. The exponential term is related to the orientation of molecules, whereas the linear term is related to the anharmonicity of the vibrations. From a fitting procedure for the band we obtained that for $A = 191(3)$ $cm^{-1}$, $\Gamma_0 = 257(75)$ $cm^{-1}$ and $B = 0.06(2)$ $cm^{-1}$ $K^{-1}$. A high slope $B$ indicates that the linear behaviour of the band linewidth of $MgB_2$ is dominated by anharmonic effects. The large anharmonicity is likely to be induced by nonlinear coupling of the $E_{2g}$ phonon to the electronic system [12, 21, 31].

On the other hand, one can see that there is an apparent temperature shift of the $E_{2g}$ peak with 35 $cm^{-1}$ to higher energies (blue shift) between room temperature and 83 K (figure 7). This result is higher than the results of [31], where the temperature shift of the $E_{2g}$ peak is almost 20 $cm^{-1}$ to high energies between room temperature and 5 K, and contradicts the results of [34] where the $E_{2g}$ mode was reported to have almost no shift with temperature for the $E_{2g}$ peak down to 15 K, a discrepancy which may be due to the differences of the grain size and the related surface energy (see below). Generally, as the temperature decreases the lattice will be compressed, and therefore an increase in the vibration frequency will be observed. This can be described by the Grüneisen relation:

$$\frac{\delta\omega}{\omega} = -\gamma\frac{\delta V}{V} \tag{3}$$

where $\omega$ is the vibration frequency, $V$ is the related cell volume, $\delta\omega$ and $\delta V$ are the vibrations of $\omega$ and $V$ due to temperature change, and $\gamma$ is a constant of about 2.9 [20, 21]. Using the

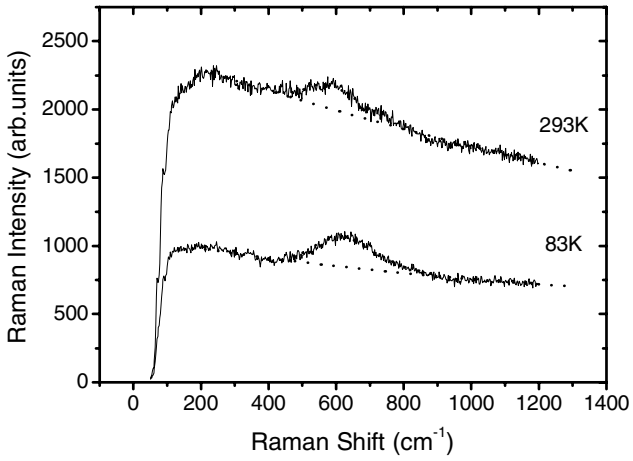


**Figure 6.** Raman spectra of $MgB_2$ at temperatures 293 and 83 K. The solid curve represents the measurement data and the dotted lines are the fitting results with a linear background and a Gaussian peak.

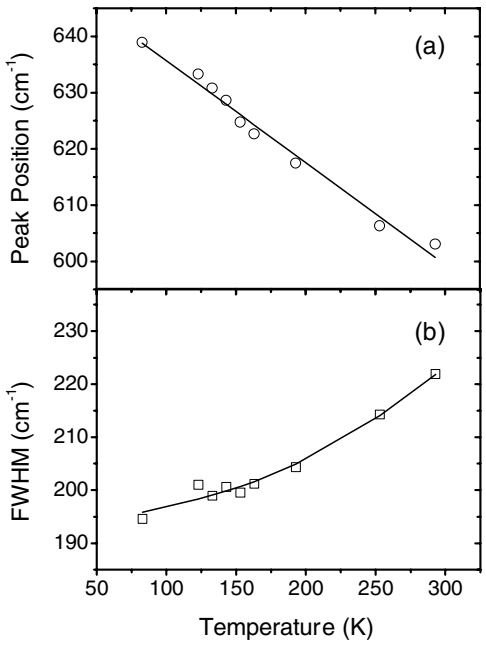


**Figure 7.** The temperature dependences of the Raman frequency and linewidth (the full width at half-maximum, FWHM) of $MgB_2$. Points are experimental frequencies and linewidths from fits of the spectra. The solid line is a theoretical fit with the formula (a) $f = aT + b$ for the peak position, where $a = -0.181(9)$ cm$^{-1}$ K$^{-1}$, $b = 653(2)$ cm$^{-1}$, and (b) $\Gamma = A + BT + \Gamma_0 \exp(-E_a/k_B T)$ (see the text).

temperature-dependent cell volume $V$ in figure 4, one can calculated the temperature-related shift and can compare it with the measured values. From figure 4, it can be obtained that $\delta V/V \approx 0.005$, while the temperature increases from 80 to 300 K. According to equation (3), one obtains the largest possible blue shift of 8.7 cm$^{-1}$. From room temperature to 80 K the measured blue shift is 39.8 cm$^{-1}$ for the $MgB_2$ sample. It is clear that the measured blue shifts were much larger than that predicted by the Grüneisen relation.

This result shows that other factors are responsible for the blue shift. It is well known that Raman spectroscopy is very sensitive to local atomic structure and to the orbital orientation. There are two other mechanisms that could induce the temperature shift of the $E_{2g}$ mode. The first one is the free-carrier-induced effects and the large coupling of the electronic system to a distinct phonon mode possibly not only accounting for the high $T_c$ and the large Raman linewidth but also accounting for the shift of this mode [18, 31]. On this basis, the smaller

pressure dependence of the $E_{2g}$ mode damping and the relative linewidth drops have been attributed to the reduction of the electron–phonon coupling constant with pressure [21]. However, on the basis of this mechanism, it is hard to understand the discrepancy of the Raman shift and the linewidth changes reported by different authors. As an example, as mentioned above, the temperature shift reported for the $E_{2g}$ peak is almost 20 $cm^{-1}$ to high energies between room temperature and 5 K in [31], and contradicts the results of [34] where the $E_{2g}$ mode was reported to have almost no shift with temperature for the $E_{2g}$ peak down to 15 K. In this work, an apparent temperature shift of the $E_{2g}$ peak with 35 $cm^{-1}$ to higher energies (blue shift) between room temperature and 83 K is observed.

It should be noted that change of the Raman band parameters, i.e. a shift of the peak position and a change of the related half-width, with grain size has been widely observed in nanometric crystals, e.g. in Si [35], GaP [36], $Sn_2P_2S_6$ [37]. In the Raman spectrum, the crystalline component broadens and its maximum clearly shifts towards lower frequency with decreasing crystalline size of silicon [35]. In this work, the average $MgB_2$ grain size obtained by x-ray diffraction analysis (see above) is about 45 nm. Therefore another mechanism, namely the grain size effect and the related surface effect, can be introduced for an explanation of the Raman peak shift and the linewidth change with the temperature decrease. For the grain size effect of nanometric crystals, the energy gap between the highest occupied orbital and the lowest unoccupied orbital levels increases as the grain size decreases [38]. As the temperature decreases, the grain size decreases further and the energy gap enlarges. Moreover, for the surface effect, the lattice distortion increases and the lattice parameters decrease due to the large surface strain, resulting in bond shortening, especially for the first and the second surface layers. The related Raman peak will shift upwards to high energy due to bond shortening. When the temperature changes, both the bond length and the surface strain will be changed and therefore a blue shift of the Raman spectrum is caused.

Although at present the quantitative relationship of the temperature effects of the grain size and the related surface of the nanometric $MgB_2$ on the Raman peak shift and the linewidth change cannot be unambiguously given, the effect caused by the grain size is indeed one of the mechanisms causing the Raman peak shift and linewidth change. Because the grain sizes obtained by different methods may be different, this mechanism may be regarded as one of the ways to understand the discrepancies among the positions of the $E_{2g}$ peak and the temperature-dependent $E_{2g}$ peak change reported by different authors (e.g. in [31] and [34]). On this basis, the position of the $E_{2g}$ peak will be moved to a low wavenumber, while the grain sizes become large, as observed by Bohnen *et al* [18] for 10 $\mu$m grains, where the position is at 580 $cm^{-1}$. If it is supposed that the temperature dependence of the peak position is linear, one can obtain a peak position at about 645 $cm^{-1}$ for 45 nm grains at 45 K from this work, which is higher than the result of 620 $cm^{-1}$ for 0.15–0.3 $\mu$m grains reported by Chen *et al* [11]. Of course, this needs further experiments to examine the correlation between the grain size, especially that on the nanometric scale, and the frequency and linewidth of the Raman peak. It is worth noticing that the difference in $MgB_2$ grain sizes is widely observed and is regarded as one of the reasons for the widely varying resistivity of $MgB_2$ samples [39].

In summary, we have examined polycrystalline $MgB_2$ samples by means of low temperature XRD and Raman scattering. The grain size determined by means of XRD is around 45 nm for both [100] and [001] directions. There is no evidence for any structural transition while the temperature decreases from 300 to 12 K. An anomalous Raman band at 603 $cm^{-1}$ is observed, which is consistent with theoretical prediction for the $E_{2g}$ in-plane boron stretching mode. The Raman frequency increases and the linewidth decreases as the temperature decreases. It is suggested that the grain size effect of $MgB_2$ on the nanometric scale will have a clear influence on the frequency and the linewidth of the Raman spectrum.

## Acknowledgments

This project was financially supported by the Ministry of Science and Technology of China (NKBRSF-G1999064603), and the National Science Foundation of China, Grant No 10174071.

## References

[1] Nagamatsu J, Nakagawa N, Muranaka T, Zenitani Y and Akimitsu J 2001 *Nature* **410** 63
[2] An J M and Pickett W E 2001 *Phys. Rev. Lett.* **86** 4366
[3] Kong Y, Dolgov O V, Jepsen O and Andersen O K 2001 *Phys. Rev.* B **64** 020501
[4] Yildirim T, Gulseren O, Lynn J W, Brown C M, Udovic T J, Huang Q, Rogado N, Hayward M A and Slusky J S 2001 *Phys. Rev. Lett.* **87** 037001
[5] Takahashi T, Sato T, Souma S, Muranaka T and Akimitsu J 2001 *Phys. Rev. Lett.* **86** 4915
[6] Rubio-Bollinger G, Suderow H and Vieira S 2001 *Phys. Rev. Lett.* **86** 5582
[7] Bud'ko S L, Lapertot G, Petrovic C, Cunningham C E, Anderson N and Canfield P C 2001 *Phys. Rev. Lett.* **86** 1877
[8] Hinks D G, Claus H and Jorgensen J D 2001 *Nature* **411** 457
[9] Osborn R, Goremychkin E A, Kolesnikov A I and Hinks D G 2001 *Phys. Rev. Lett.* **87** 017005
[10] Jin R, Paranthaman M, Zhai H Y, Christen H M, Christen D K and Mandrus D 2001 *Phys. Rev.* B **64** 220506
[11] Chen X K, Konstantinovic M J, Irwin J C, Lawrie D D and Franck J P 2001 *Phys. Rev. Lett.* **87** 157002
[12] Liu A Y, Mazin I I and Kortus J 2001 *Phys. Rev. Lett.* **87** 087005
[13] Souma S, Machida Y, Sato T, Takahashi T, Matsui H, Wang S-C, Ding H, Kaminski A, Campuzano J C, Sasaki S and Kadowaki K 2003 *Nature* **423** 65
[14] Gonnelli R S, Daghero D, Ummarino G A, Stepanov V A, Jun J, Kazakov S M and Karpinski J 2002 *Phys. Rev. Lett.* **89** 247004
[15] Bugoslavsky Y, Miyoshi Y, Perkins G K, Berenov A V, Lockman Z, MacManus-Driscoll J L, Cohen L F, Caplin A D, Zhai H Y, Paranthaman M P, Christen H M and Blarnire M 2002 *Supercond. Sci. Technol.* **15** 526
[16] Choi H J, Roundy D, Sun H, Cohen M L and Louie S G 2001 *Nature* **418** 758
[17] Klein M V and Dierker S B 1984 *Phys. Rev.* B **29** 4976
Dierker S B and Klein M V 1983 *Phys. Rev. Lett.* **50** 853
Devereaux T P, Einzel D, Stadlober B, Hackl R, Leach D H and Nevmeier J J 1994 *Phys. Rev. Lett.* **72** 396
[18] Bohnen K-P, Heid R and Renker B 2001 *Phys. Rev. Lett.* **86** 5771
[19] Kunc K, Loa I, Syassen K, Kremer R K and Ahn K 2001 *J. Phys.: Condens. Matter* **13** 9945
[20] Goncharov A F, Struzhkin V V, Gregoryanz E, Hu J, Hemley R J, Mao H-K, Lapertot G, Bud'ko S L and Canfield P C 2001 *Phys. Rev.* B **64** 100509(R)
[21] Goncharov A F and Struzhkin V V 2003 *Physica* C **385** 117
[22] Young R A, Mackie P E and von Dreele R B 1977 *J. Appl. Crystallogr.* **10** 262
[23] Cava R J, Zandbergen H W and Innmaru K 2003 *Physica* C **385** 8
[24] Yang D, Sun H, Lu H, Guo Y, Li X and Hu X 2003 *Supercond. Sci. Technol.* **16** 576
[25] Jones M E and Marsh R E 1954 *J. Am. Chem. Soc.* **76** 1434
[26] Chen K, Ma P, Nie R J, Yang T, Xie F X, Liu L Y, Wang S Z, Dai Y D and Wang F 2002 *Supercond. Sci. Technol.* **15** 1721
[27] Jorgensen J D, Hinks D G and Short S 2001 *Phys. Rev.* B **63** 224522
[28] Lonnberg B 1988 *J. Less-Common Met.* **141** 145
[29] Vogt T, Schneider G, Hriljac J A, Yang G and Abell J S 2001 *Phys. Rev.* B **63** 220505
[30] Hlinka J, Gregora I, Pokorný J, Plecenik A, Kúš P, Satrapinsky L and Beňačka Š 2001 *Phys. Rev.* B **64** 140503
[31] Rafailov P M, Dworzak M and Thomsen C 2002 *Solid State Commun.* **122** 455
[32] Carabotos-Nédelec C and Becker P 1997 *J. Raman Spectrosc.* **28** 663
[33] Born M and Huang K 1968 *Dynamical Theory of Crystal Lattice* (Oxford: Clarendon)
[34] Martinho H, Martin A A, Rettori C, de Lima O F, Ribeiro R A, Avila M A, Pagliuso P G and Moreno N O 2001 *Preprint* cond-mat/0105204
[35] Veprek S, Iqbal Z, Oswald H R and Webb A P 1981 *J. Phys. C: Solid State Phys.* **14** 295
[36] Hayashi S and Yamamoto K 1986 *Superlatt. Microstruct.* **2** 581
[37] Gomonnai A V, Azhniuk Yu M, Vysochanskii Yu M, Kikinshi A A, Kis-Varga M, Daroczy L, Prits I P and Voynarovych I M 2003 *J. Phys.: Condens. Matter* **15** 6381
[38] Ball P and Garwin L 1992 *Nature* **355** 761
[39] Rowell J M 2003 *Supercond. Sci. Technol.* **16** R17